Hole-Induced Avalanche and its Role in Dark Current in SPADs

Isobel Nicholson*, Gabriel Mugny†, Remi Helleboid‡, Bastien Mamdy†, Dominique Golanski†, Sebastien Place†, Patryk Maciazek*, Denis Rideau†
*STMicroelectronics Edinburgh, UK, †STMicroelectronics Crolles, France, ‡University of Paris-Saclay, France.

***Abstract*— Dark count rate in SPAD is difficult to predict in TCAD. A newly proposed simulation methodology combining multi-phonon carrier generation and high statistics empirical Monte-Carlo breakdown probability is presented here, showing good agreement with measured data for a variety of SPADs. The dark counts are shown to be induced by holes generated at the silicon/oxide surface interface.**

Index Terms— SPAD, DCR, Dark current, Monte-Carlo, TCAD, Multi-phonon, Avalanche.

I. Introduction

Single-photon avalanche diodes (SPADs) are PN junctions reverse biased beyond their breakdown voltage. When a photo-generated charge carrier reaches the high electric field across the junction, it causes an avalanche of impact ionization (II) events. This measurable current pulse is terminated when the voltage across the SPAD falls back below breakdown and the device is subsequently reset. These devices are useful for time of flight applications due to their exceptional timing characteristics. Recently very small SPADs have been made, allowing high resolution applications [1-2]. Size reduction requires shrinking of the guard ring, which prevents edge effects.

Dark count rate (DCR) is a significant challenge for the SPAD, with hundreds of false counts per second degrading the signal. Considering defects associated to interfaces neutralized by successful passivation, a remaining contributor to DCR can be associated to high voltage in the SPAD. The ability to predict this DCR would be of great benefit, allowing rapid development towards low DCR SPADs. Previous attempts to understand its origin with simulation have proposed that it is due to contamination from critical SPAD implanted wells [3]. In this study we establish a simulation methodology which supports hole-induced avalanche current from the surface interface of the SPAD.

II. Device Description

To avoid high electric field leading to lateral II or tunneling between the anode and cathode of a SPAD, it is necessary to grade the doping along the silicon/oxide surface interface. The lateral junction thus implemented leaves an unpassivated area in its space charge region. Four SPADs were constructed with equal ratios of passivated to unpassivated surface area but varying ratios of guard ring to junction area as shown in fig. 1a-b).

The DCR of these SPADs varies with voltage, transitioning to exponentially increasing DCR at a threshold voltage which was measured in fig. 1c) to be inversely correlated with the size of the guard ring. The SPADs are simulated with a well-calibrated TCAD process and device engine to obtain their electric fields at a variety of voltages. There are two conditions required for the origin of the DCR to be from holes on the surface interface of the SPAD: 1) an electric field high enough to stimulate hole generation near the surface interface and 2) a non-zero breakdown probability (BrP) from the surface.

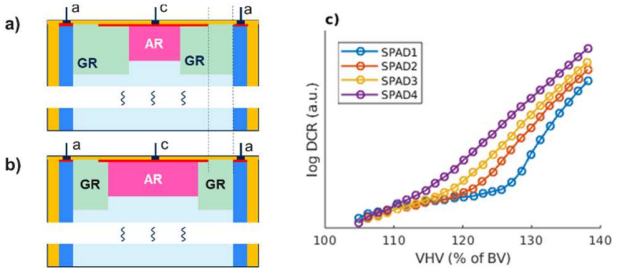

Fig. 1. The SPAD constitutes an avalanche region (AR), and a guard ring (GR) which conducts the anode voltage to the AR while minimizing electric field at the surface. a) SPAD1 has a small AR and large GR in comparison to b) SPAD4 with an aggressive/small GR. SPADs 2 and 3 vary linearly between SPADs 1 and 4. The passivated surface area (red) is constant for all SPADs. c) The DCR at 60°C shows at a high voltage (VHV) characteristic exacerbated by GR reduction. Abbreviations: a: anode, c: cathode.

III. Breakdown Modelling

A. Monte-Carlo simulation

The BrP is modelled using the Drift-Diffusion Monte-Carlo (DDMC) simulation engine presented in [4]. This tool is well calibrated for jitter and photo-generated BrP. The carrier drift and diffusion is governed by the Boltzmann equation and Einstein relation,

$$\frac{\partial y}{\partial t} = -\mu F \frac{\partial y}{\partial x} + \frac{k_B T \mu}{q} \frac{\partial^2 y}{\partial x^2} \quad (1)$$

where μ is mobility; F is the electric field; k_B is the Boltzmann constant; T is the temperature and q is the electron charge. Cumulative II probability is driven by the van

Overstraetan-de Man model. The device is biased at a fixed potential. To establish whether a defect-generated carrier could be a plausible source of a dark count, we launch simulations for holes and electrons respectively from each point in the device.

As the BrP from the unpassivated regions is low it is necessary to run significant numbers of simulations. We ran 300 simulations per point on a 10nm grid covering the edge of the unpassivated region. The simulations are repeated for different values of fixed surface charge concentration on the silicon/oxide interface: 1e10cm^{-2}, 1e11cm^{-2} and 1e12cm^{-2}. We define an avalanche as 50 II events to ensure reasonable simulation time and memory requirements. All simulations are performed at 60°C.

B. Results

With the DDMC engine, there is no breakdown from the unpassivated surface for electrons. However it is possible to find a low BrP extending 100nm into the region for holes. Fig. 2) shows the BrP maps. Fig. 3) shows some characteristic trajectories of these carriers through the guard ring.

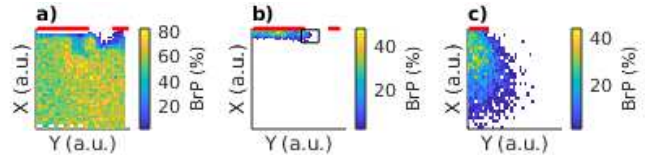

Fig. 2. BrP maps for avalanches initiated by a) electrons and b-c) holes. The map is shown for half of SPAD1 at 25V. Fig 2c) is a zoom of b) covering the area indicated by the box in b), i.e. the edge of the passivated region at the surface. Passivated surface area is indicated in red.

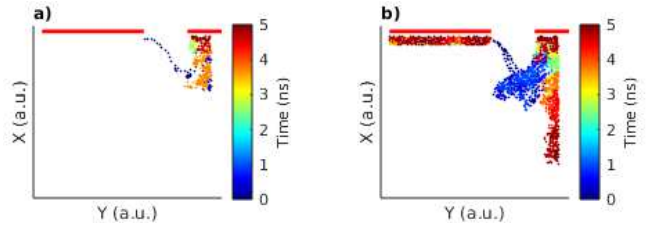

Fig. 3. A hole 30nm from the edge of the passivated region indicated by the red bar can be a) safely evacuated or b) lead to II events. Holes and electrons position are logged every ps and coloured by time since their creation.

The fixed surface charge changes the shape of the electric field in the lower doped regions, driving changes in the BrP characteristics. While the peak electric field value near the surface is reduced, the region of high electric field is extended. Since non-zero breakdown probability can occur for even relatively low fields if the region is large enough, this should be taken into account during guard ring design. Within the first 60nm of the surface, the average breakdown probability varies with the guard ring size and fixed surface charge, see fig. 4. No exacerbation of unpassivated breakdown is seen within the first 60nm in this case. A protective effect can be observed in the passivated region.

The voltage dependence of the breakdown probability in the unpassivated region within 60nm of the surface is shown in fig. 5. The dependence is exponential indicating that this is a plausible candidate to explain the measured DCR. In all cases the most aggressive guard ring displays the high BrP.

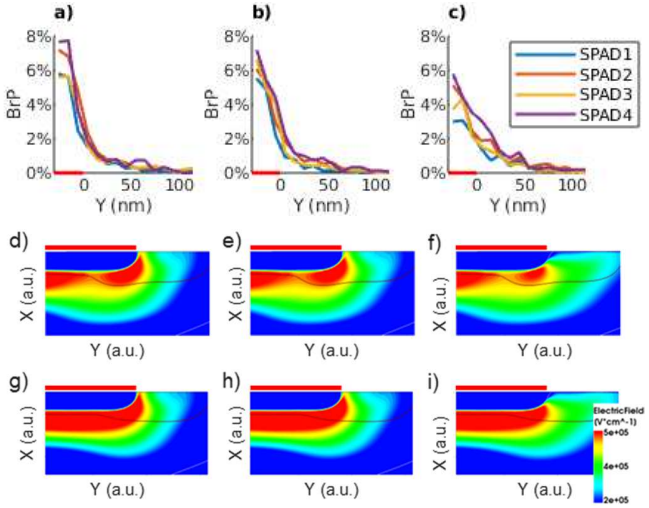

Fig. 4. BrP for holes launched within 60nm of the surface for surface fixed charge concentration of a) 1e10 cm^{-2}, b) 1e11 cm^{-2} and c) 1e12 cm^{-2}. In all cases, there is a non-zero BrP outside of the passivated region indicated by the red line. The corresponding electric fields shown for SPAD1 (d-f) and SPAD4 (h-i) at 25V illustrate the fixed surface charge effect.

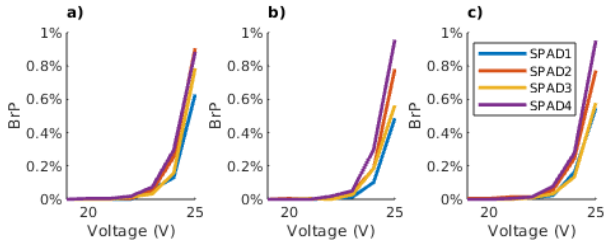

Fig. 5. Voltage dependence of the average breakdown probability of unpassivated surface within 60nm of the surface for a fixed surface charge of a) 1e10 cm^{-2}, b) 1e11 cm^{-2} and c) 1e12 cm^{-2}.

C. Negative Charge Densities

It is possible for negative charge densities to occur on a silicon/oxide interface when nitride is present nearby. For a similar order of magnitude from -1e10 cm^{-2} to -1e12 cm^{-2}, the effect is opposite to the positive charge density, exacerbating the high electric field near the surface outside the passivated region (fig. 6). For charge interface concentrations as high as -1e12 cm^{-2} the increase in electric field is catastrophic, leading to breakdown probabilities of > 20% outside of the passivated region on all guard ring designs. Even at -1e11 cm^{-2} there is a modest degradation. The voltage dependence of the average unpassivated BrP within 60nm of the surface for -1e12 cm^{-2} becomes linear (fig. 7) but remains exponential for lower values.

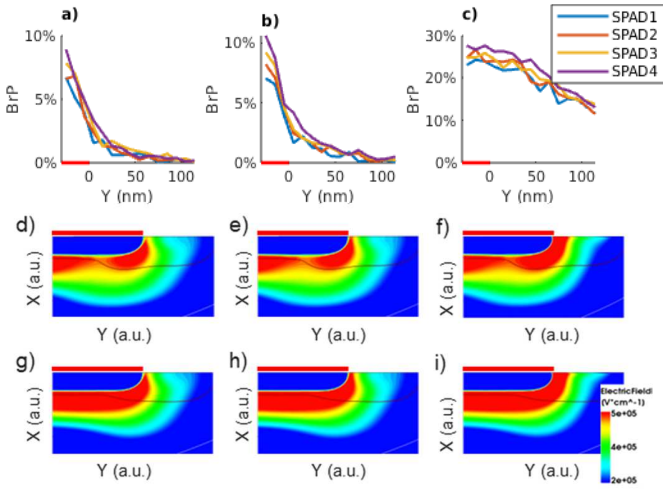

Fig. 6. BrP for holes launched within 60nm of the surface for surface fixed charge concentration of a) -1e10 cm^{-2}, b) -1e11 cm^{-2} and c) -1e12 cm^{-2}. In all cases, there is a non-zero BrP outside of the passivated region indicated by the red line. The corresponding electric fields shown for SPAD1 (d-f) and SPAD 4 (g-i) at 25V illustrate the fixed surface charge effect.

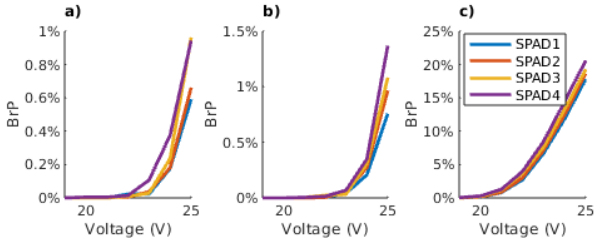

Fig. 7. Voltage dependence of the average breakdown probability of unpassivated surface within 60nm of the surface for a fixed surface charge of a) -1e10 cm^{-2}, b) -1e11 cm^{-2} and c) -1e12 cm^{-2}.

D. McIntyre model

A popular alternative to DDMC for breakdown probability modelling is the McIntyre model [5]. This model is typically used along the electric field lines, simplifying a 2- or 3- dimensional problem into a series of 1D problems. However this implicitly assumes that no diffusion takes place and carriers move strictly along the electric field lines. This fundamental limitation can cause BrP originating low or rapidly changing electric field locations to be missed. This is indeed the case in the current study, where no BrP from the unpassivated region is predicted by the McIntyre model. The exception to this is for -1e12 cm^{-2} fixed surface charge, where the field is sufficiently high to drive BrP from the area directly without diffusion (fig. 8). This highlights the benefit of diffusion-based modelling tools for DCR prediction.

IV. Generation at the Interface

A. Multi-phonon model

The capture/emission rate of carriers due to defects are described here in the framework of a multi-phonon

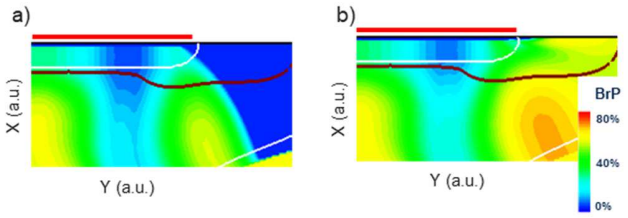

Fig. 8. The BrP from the McIntyre model for a fixed surface charge of a) -1e10 cm^{-2} and b) -1e12 cm^{-2}. There is no BrP from the unpassivated surface (passivated area indicated by the red line) until the surface charge is increased.

approximation [6-8]. The effect of the electric field is included through the modification of the density of states (DOS), as described in [9] (fig. 9). The electric field entering the model is taken 30nm from the surface to avoid numerical discontinuity. For simplicity, only mid-band-gap donor type defects are considered and the traps are doping independent. The generation/recombination rate increases rapidly from 1e5 V/cm.

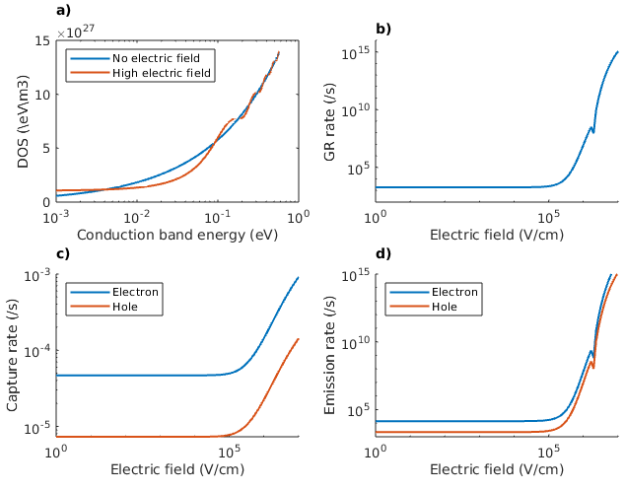

Fig. 9. a) The multi-phonon model causes oscillations in the DOS at high electric field. The resulting generation / recombination rate for a single trap (fig. 9b) is calculated from the electron and hole capture (fig. 9c) and emission (fig. 9d) rates.

B. Predicted DCR from surface

Convolving the multi-phonon generation rate with the BrP for the positive fixed surface charge fits the measured data with a trap concentration of 4e10cm^{-2} (fig. 10a). The trap concentration is varied independently of the fixed surface charge. A noise floor of 200cps is added to represent constant voltage contributions from elsewhere in the device. The model correctly captures the increase in DCR due to the weakened guard ring. The gradient may be improved with a more detailed trap profile. There is a small protective effect of increasing the fixed surface charge for SPAD1 which becomes negligible for aggressive guard rings (fig. 10b-c).

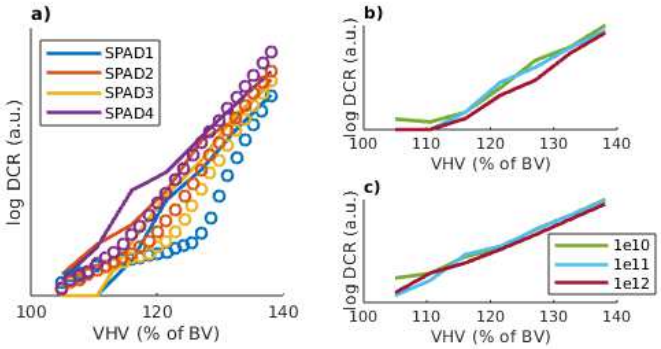

Fig. 10. a) Dark count rate comparison of predicted (lines) vs measured data (circles) for fixed surface charge of 1e11 cm^{-2}. b-c) Predicted DCR for b) SPAD1 and c) SPAD4 for varying fixed surface charge. A trap concentration of 4e10 cm^{-2} and a noise floor of 200cps is used.

In contrast, the negative fixed surface charge significantly modulates the DCR such that is necessary to individually fit the trap concentration to the measurement data for each fixed surface charge values (fig. 11).

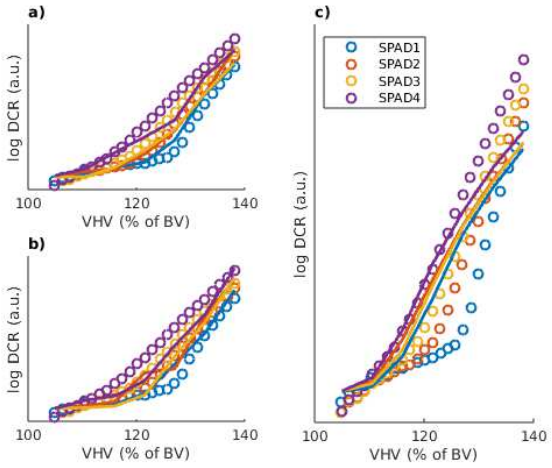

Fig. 11. Dark count rate comparison of predicted (lines) vs measured data (circles) for fixed surface charge of a) -1e10 cm^{-2}, b) -1e11 cm^{-2} and c) -1e12 cm^{-2}. Fitted trap concentration values of 7e9 cm^{-2}, 5e9 cm^{-2} and 5e6 cm^{-2} respectively were used with a noise floor of 170cps.

Appropriate fitted values are 7e9 cm^{-2}, 5e9 cm^{-2} and 5e6 cm^{-2}, for fixed surface charges densities of -1e10 cm^{-2}, -1e11 cm^{-2} and -1e12 cm^{-2} respectively. In the final case, this could reflect an unrealistically clean interface, suggesting that the trap parameters should be fitted to reduce the trap generation rate if the silicon interface was found to have this value of fixed charge . A noise floor of 170cps is also used.

The DCR methodology captures the rate of DCR increase with voltage well, especially for -1e10 cm^{-2} fixed surface charge. This case also has the largest voltage difference between the knee points of the least and most aggressive guard rings, fitting the data well. As the fixed surface charge increases, the voltage difference decreases and the gradient flattens off.

C. Design Implications

As figs 4 and 6 show, it is essential to take the fixed surface charge into account when considering electric field engineering near interfaces. It is possible to tailor guard ring designs so that they remain functional even under a high level of negative surface charge, see fig. 12). This guard ring maintains the same aggressive pitch as SPAD4. Without fixed surface charge, it performs marginally worse than the original guard ring, but the catastrophic degradation is avoided and performance is even improved when the surface charge is increased to -1e12 cm^{-2}.

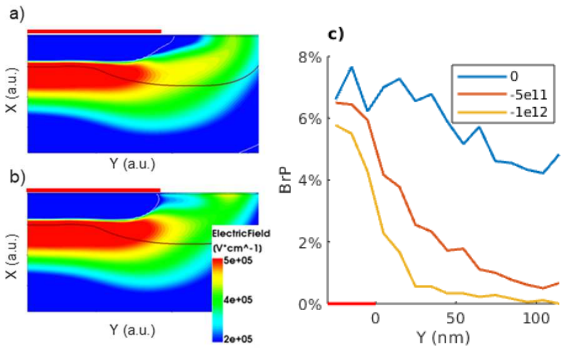

Fig. 12. Electric field in the guard ring with a fixed surface charge of a) 0 cm^{-2} and b) -1e12 cm^{-2}. The aggressive guard ring has the same dimensions as SPAD4. Average BrP within 60nm of the surface is shown in fig. 12c) for three values of fixed surface charge. The unpassivated region is indicated by red line.

V. Conclusion

In this study we proposed a novel simulation methodology to predict high voltage DCR in SPADs and describe both electron and hole-generated events. These hole-induced breakdown events are low probability and cover only a small surface area. Nevertheless, combined with multi-phonon simulations to predict generation near the surface and reasonable fitted trap concentrations of 4e10 cm^{-2} or less, this BrP is sufficient to explain the observed DCR. Fixed surface charge concentration can modulate the BrP and thus the shape of the DCR curve.

In the case of negative fixed surface charge, both the BrP and the trap generation rate are significantly increased. A guard ring design which is still functional even with significant negative fixed surface charge is presented.

References

[1] K. Morimoto et al, *Opt. Express 28*, 2020
[2] J. Ogi et al., *Sensors*, 2023
[3] M. Sicre *et al*., *ESSDERC*, 2021
[4] R. Helleboid *et al.*, *Journal of Physics D: Applied Physics*, 2022
[5] R. Helleboid *et al.*, *Solid-State Electronics*, 2022
[6] D. Garetto et al, *Solid-state electronics,* 2012
[7] W. Goes et al, *Microelectronics Reliability*, 2018
[8] C. Delerue et al, *Phys. Rev. B*, 2001
[9] A. Schenk, *Solid-State Electronics*, 1992